Z. Angew. Math. Phys. (2021) 72:154

0044-2275/21/040001-12
published online July 4, 2021
https://doi.org/10.1007/s00033-021-01584-w

Zeitschrift für angewandte Mathematik und Physik ZAMP

Variable-coefficient symbolic computation approach for finding multiple rogue wave solutions of nonlinear system with variable coefficients

Jian-Guo Liu, Wen-Hui Zhu and Yan He

Abstract. In this paper, a variable-coefficient symbolic computation approach is proposed to solve the multiple rogue wave solutions of nonlinear equation with variable coefficients. As an application, a $(2+1)$-dimensional variable-coefficient Kadomtsev–Petviashvili equation is investigated. The multiple rogue wave solutions are obtained and their dynamic features are shown in some 3D and contour plots.

Mathematics Subject Classification. 35C08, 68M07, 33F10.

Keywords. Variable-coefficient symbolic computation approach, Rogue wave, Variable-coefficient Kadomtsev–Petviashvili equation.

1. Introduction

In this paper, the following (2+1)-dimensional variable-coefficient Kadomtsev–Petviashvili (vcKP) equation is investigated [1]

$$\alpha(t)u_x^2 + \alpha(t)uu_{xx} + \beta(t)u_{xxxx} - \gamma(t)u_{yy} + u_{xt} = 0, \tag{1}$$

where $u = u(x, y, t)$ describes amplitude of the long wave of two-dimensional fluid domain on varying topography or in turbulent flow over a sloping bottom. $\alpha(t)$, $\beta(t)$ and $\gamma(t)$ are arbitrary real functions. The solitonic solution [1], Wronskian and Gramian solutions [2], Bäcklund transformation [3], breather wave solutions [4], lump and interactions solutions [5,6] of Eq. (1) have been studied.

Rogue wave has important applications in ocean's waves [7], optical fibers [8], Bose–Einstein condensates [9] and other fields. Rogue wave solutions of many integrable equations have been investigated [10–17]. Recently, a symbolic computation approach to obtain the multiple rogue wave solutions is proposed by Zhaqilao [18]. But the main application of this method is constant-coefficient integrable equation [19–21], which is not suitable for variable-coefficient integrable equation. So, we give an improved method named variable-coefficient symbolic computation approach (vcsca) to solve this problem and apply this method to Eq. (1), which will be the main work of our paper.

The organization of this paper is as follows. Section 2 proposes a vcsca; Sect. 3 gives the 1-rogue wave solutions; Sect. 4 obtains the 3-rogue wave solutions; Sect. 5 presents the 6-rogue wave solutions; and Sect. 6 gives this conclusions.

Project supported by National Natural Science Foundation of China (Grant No 81960715).

2. Modified symbolic computation approach

Here, we present a vcsca to find the multiple rogue wave solutions of variable-coefficient integrable equation

Step 1. Instead of the traveling wave transformation in Ref. [18], we make a non-traveling wave transformation $\upsilon = x - \omega(t)$ in the following nonlinear system with variable coefficients

$$\Xi(u, u_t, u_x, u_y, u_{xy}, \ldots) = 0, \tag{2}$$

and Eq. (2) is reduced to a (1+1)-dimensional equation

$$\Xi(u, u_\upsilon, u_y, u_{\upsilon y}, \ldots) = 0. \tag{3}$$

Step 2. By Painlevé analysis, we make the following transformation

$$u(\upsilon, y) = \frac{\partial^n}{\partial \upsilon^m} ln\xi(\upsilon, y). \tag{4}$$

m can be derived by balancing the order of the highest derivative term and nonlinear term.

Step 3. Assuming

$$\xi(\upsilon, y) = F_{n+1}(\upsilon, y) + 2\nu y P_n(\upsilon, y) + 2\mu\upsilon Q_n(\upsilon, y) + (\mu^2 + \nu^2)F_{n-1}(\upsilon, y), \tag{5}$$

with

$$\begin{aligned}
F_n(\upsilon, y) &= \sum_{k=0}^{n(n+1)/2} \sum_{i=0}^{k} a_{n(n+1)-2k,2i} y^{2i} \upsilon^{n(n+1)-2k}, \\
P_n(\upsilon, y) &= \sum_{k=0}^{n(n+1)/2} \sum_{i=0}^{k} b_{n(n+1)-2k,2i} \upsilon^{2i} y^{n(n+1)-2k}, \\
Q_n(\upsilon, y) &= \sum_{k=0}^{n(n+1)/2} \sum_{i=0}^{k} c_{n(n+1)-2k,2i} y^{2i} \upsilon^{n(n+1)-2k},
\end{aligned}$$

$F_0 = 1, F_{-1} = P_0 = Q_0 = 0$, where $a_{m,l}$, $b_{m,l}$ and $c_{m,l}(m, l \in [0, 2, 4, \ldots, n(n+1)])$ are unknown constants, μ and ν are the wave center.

Step 4. Substituting Eqs. (4) and (5) into Eq. (3) and equating all the coefficients of the different powers of υ and y to zero, we can know $a_{m,l}, b_{m,l}$ and $c_{m,l}(m, l \in [0, 2, 4, \ldots, n(n+1)])$. The corresponding multiple rogue wave solutions can be presented.

3. 1-Rogue wave solutions

Based on the vcsca, set

$$\alpha(t) = \frac{6\beta(t)}{\Theta_0}, \upsilon = x - \omega(t), u = 2\Theta_0 \left[ln\xi(\upsilon, y)\right]_{\upsilon\upsilon}, \tag{6}$$

and Eq. (1) can be changed as

$$\begin{aligned}
&6\xi_\upsilon^2[\xi[3\beta(t)\xi_{\upsilon\upsilon\upsilon\upsilon} - 2\omega'(t)\xi_{\upsilon\upsilon}] + 3\beta(t)\xi_{\upsilon\upsilon}^2] + 2\xi^2\xi_\upsilon[2\omega'(t)\xi_{\upsilon\upsilon\upsilon} \\
&\quad -3\beta(t)\xi_{\upsilon\upsilon\upsilon\upsilon\upsilon}] + \xi[\xi[-3\beta(t)\xi_{\upsilon\upsilon\upsilon\upsilon}\xi_{\upsilon\upsilon} + 2\beta(t)\xi_{\upsilon\upsilon\upsilon}^2 + 3\omega'(t)\xi_{\upsilon\upsilon}^2] \\
&\quad +\xi^2[\beta(t)\xi_{\upsilon\upsilon\upsilon\upsilon\upsilon\upsilon} - \omega'(t)\xi_{\upsilon\upsilon\upsilon\upsilon}] - 6\beta(t)\xi_{\upsilon\upsilon}^3] - 24\beta(t)\xi_{\upsilon\upsilon\upsilon}\xi_\upsilon^3 \\
&\quad +\gamma(t)[[6\xi_\upsilon^2 - 2\xi\xi_{\upsilon\upsilon}]\xi_y^2 + 2\xi[\xi\xi_{\upsilon\upsilon y} - 4\xi_\upsilon\xi_{\upsilon y}]\xi_y + \xi[\xi_{yy}[\xi\xi_{\upsilon\upsilon} - 2\xi_\upsilon^2] \\
&\quad +\xi[2\xi_{\upsilon y}^2 + 2\xi_\upsilon\xi_{\upsilon yy} - \xi\xi_{\upsilon\upsilon yy}]]] + 6\omega'(t)\xi_\upsilon^4.
\end{aligned} \tag{7}$$

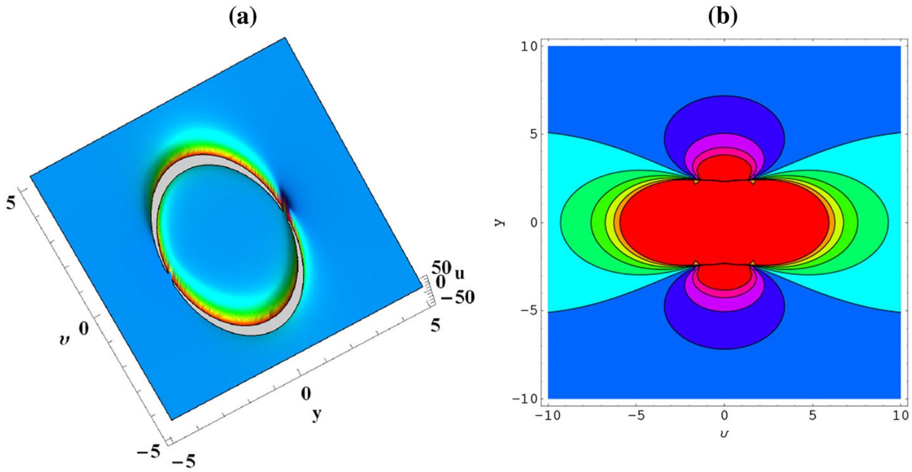

FIG. 1. Rogue wave (10) with $\mu = \nu = 0$, $\Theta_0 = 1$, $\zeta_0 = -10$, $\zeta_1 = 2$, **a** 3D graphic, **b** contour plot

According to Eq. (5), we have

$$\xi(\upsilon, y) = (\upsilon - \mu)^2 + \zeta_1(y - \nu)^2 + \zeta_0, \tag{8}$$

where μ, ν, ζ_0 and ζ_1 are unknown real constants. Substituting Eq. (8) into Eq. (7) and equating the coefficients of all powers υ and y to zero, we obtain

$$\gamma(t) = \frac{3\beta(t)}{\zeta_0\zeta_1}, \omega'(t) = \zeta_1\gamma(t). \tag{9}$$

Substituting Eqs. (8) and (9) into Eq. (6), the 1-rogue wave solutions for Eq. (1) can be read as

$$u = \frac{4\Theta_0[-(\mu - \upsilon)^2 + \zeta_1(y - \nu)^2 + \zeta_0]}{[(\mu - \upsilon)^2 + \zeta_1(y - \nu)^2 + \zeta_0]^2}. \tag{10}$$

When $\zeta_0 > 0$, rogue wave (10) has three extreme value points (μ, ν), $(\mu \pm \sqrt{3}\sqrt{\zeta_0}, \nu)$. When $\zeta_0 < 0, \zeta_1 > 0$, rogue wave (10) has three extreme value points (μ, ν), $(\mu, \nu \pm \frac{\sqrt{-\zeta_0}}{\sqrt{\zeta_1}})$. Figures 1 and 2 describe the dynamic features of rogue wave (10) when ζ_0 and ζ_1 select different values.

4. 3-Rogue wave solutions

In order to look for the 3-rogue wave solutions, we set

$$\begin{aligned}\xi(\upsilon, y) = {} & \mu^2 + \nu^2 + \upsilon^6 + y^6\zeta_{17} + y^4\zeta_{16} + 2\mu\upsilon\left(y^2\zeta_{23} + \upsilon^2\zeta_{24} + \zeta_{22}\right) \\ & + 2\nu y\left(y^2\zeta_{20} + \upsilon^2\zeta_{21} + \zeta_{19}\right) + \upsilon^4 y^2\zeta_{11} + y^2\zeta_{15} \\ & + \upsilon^2\left(y^4\zeta_{14} + y^2\zeta_{13} + \zeta_{12}\right) + \upsilon^4\zeta_{10} + \zeta_{18},\end{aligned} \tag{11}$$

where $\zeta_i (i = 10, \ldots, 24)$ is unknown real constant. Substituting Eq. (11) into Eq. (7) and equating the coefficients of all powers υ and y to zero, we get

$$\gamma(t) = \frac{90\beta(t)}{\zeta_{13}}, \omega'(t) = \frac{30\zeta_{11}\beta(t)}{\zeta_{13}}, \zeta_{14} = \frac{\zeta_{11}^2}{3}, \zeta_{16} = \frac{17\zeta_{11}\zeta_{13}}{270},$$

$$\zeta_{20} = -\frac{1}{9}\zeta_{11}\zeta_{21}, \zeta_{17} = \frac{\zeta_{11}^3}{27}, \zeta_{15} = \frac{19\zeta_{13}^2}{108\zeta_{11}}, \zeta_{23} = -\zeta_{11}\zeta_{24},$$

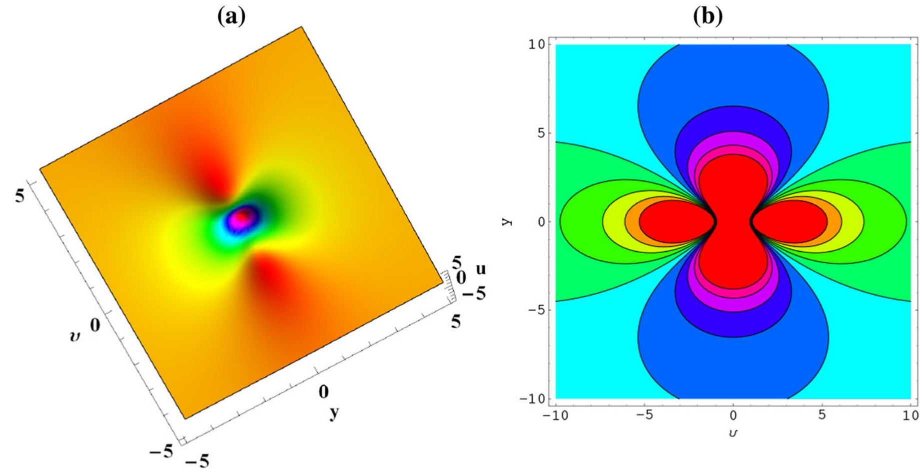

FIG. 2. Rogue wave (10) with $\mu = \nu = 0$, $\Theta_0 = 1$, $\zeta_0 = 1$, $\zeta_1 = 2$, **a** 3D graphic, **b** contour plot

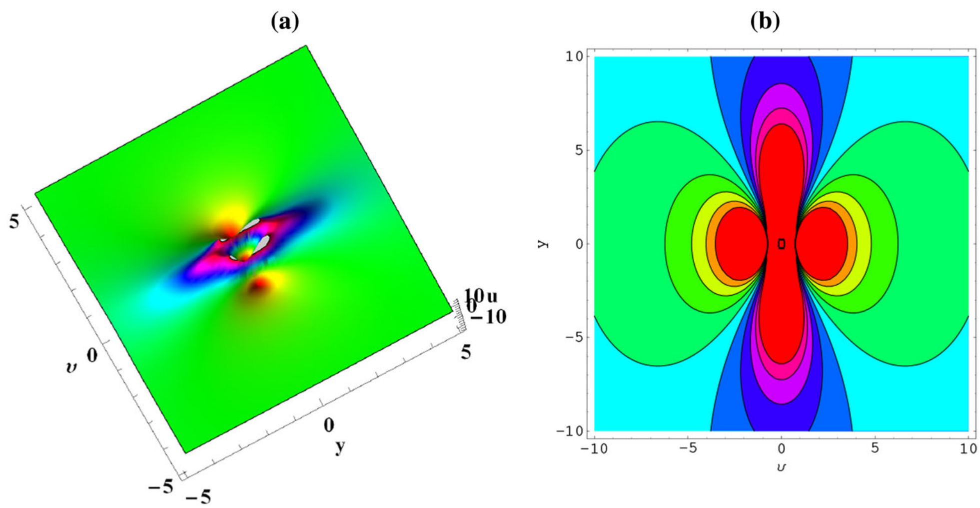

FIG. 3. Rogue wave (13) with $\mu = \nu = 0$, $\Theta_0 = 1$, $\zeta_{11} = \zeta_{13} = \zeta_{21} = \zeta_{24} = 1$, **a** 3D graphic, **b** contour plot

$$\begin{aligned}\zeta_{22} &= -\frac{\zeta_{13}\zeta_{24}}{30\zeta_{11}}, \zeta_{12} = -\frac{5\zeta_{13}^2}{36\zeta_{11}^2}, \zeta_{10} = \frac{5\zeta_{13}}{6\zeta_{11}}, \zeta_{19} = \frac{\zeta_{13}\zeta_{21}}{18\zeta_{11}},\\ \zeta_{18} &= -\mu^2 - \nu^2 + \mu^2\zeta_{24}^2 + \frac{\nu^2\zeta_{21}^2}{3\zeta_{11}} + \frac{5\zeta_{13}^3}{72\zeta_{11}^3}.\end{aligned} \tag{12}$$

Substituting Eqs. (11) and (12) into Eq. (6), the 3-rogue wave solutions for Eq. (1) can be read as

$$\begin{aligned}u = {}&[24\Theta_0\zeta_{11}[5[12y^4\zeta_{11}^4 + 36\zeta_{11}^2\left(15\upsilon^4 + y^2\zeta_{13} + 2\nu y\zeta_{21} + 6\mu\upsilon\zeta_{24}\right)\\ &+216\upsilon^2y^2\zeta_{11}^3 + 180\upsilon^2\zeta_{13}\zeta_{11} - 5\zeta_{13}^2][40y^6\zeta_{11}^6 + 360\upsilon^2y^4\zeta_{11}^5\\ &+2\zeta_{11}^2[95y^2\zeta_{13}^2 + 6\zeta_{13}\left(75\upsilon^4 + 10\nu y\zeta_{21} - 6\mu\upsilon\zeta_{24}\right) + 180\nu^2\zeta_{21}^2]\\ &+4y^2\zeta_{11}^4[y\left(17y\zeta_{13} - 60\nu\zeta_{21}\right) + 270\upsilon\left(\upsilon^3 - 2\mu\zeta_{24}\right)] + 1080\zeta_{11}^3[\upsilon^2y^2\zeta_{13}\end{aligned}$$

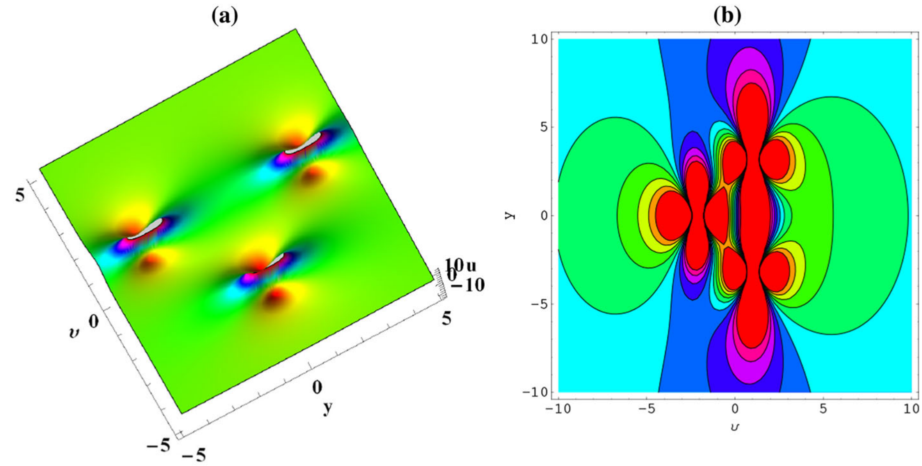

FIG. 4. Rogue wave (13) with $\mu = 10, \nu = 0$, $\zeta_{11} = \zeta_{13} = \zeta_{21} = \zeta_{24} = 1$, $\Theta_0 = 1$, **a** 3D graphic, **b** contour plot

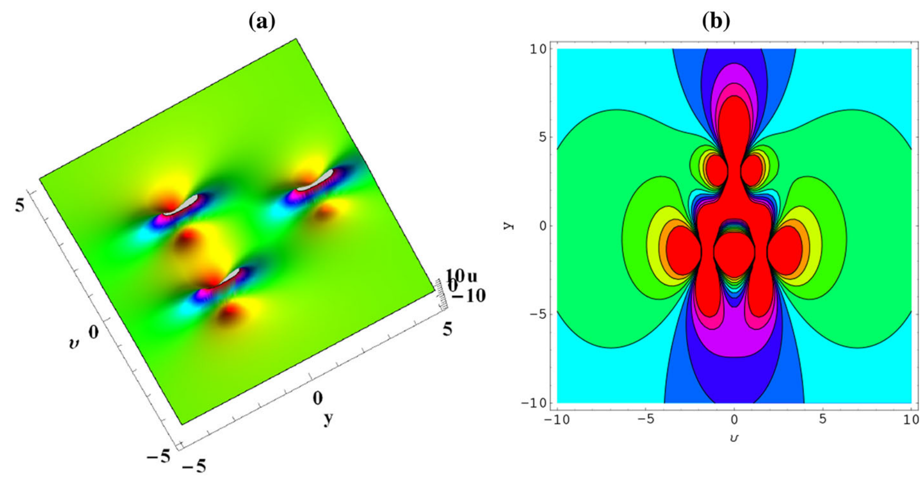

FIG. 5. Rogue wave (13) with $\mu = 0, \nu = 10$, $\zeta_{11} = \zeta_{13} = \zeta_{21} = \zeta_{24} = 1$, $\Theta_0 = 1$, **a** 3D graphic, **b** contour plot

$$
\begin{aligned}
&+2\nu\upsilon^2 y\zeta_{21} + \left(\upsilon^3 + \mu\zeta_{24}\right)^2] - 150\upsilon^2\zeta_{13}^2\zeta_{11} + 75\zeta_{13}^3] - 12\zeta_{11}[60\upsilon y^4\zeta_{11}^4 \\
&+180\upsilon\zeta_{11}^2\left(3\upsilon^4 + y^2\zeta_{13} + 2\nu y\zeta_{21} + 3\mu\upsilon\zeta_{24}\right) + 180y^2\zeta_{11}^3\left(2\upsilon^3 - \mu\zeta_{24}\right) \\
&+6\zeta_{13}\zeta_{11}\left(50\upsilon^3 - \mu\zeta_{24}\right) - 25\upsilon\zeta_{13}^2]^2]]/[[40y^6\zeta_{11}^6 + 360\upsilon^2 y^4\zeta_{11}^5 \\
&+2\zeta_{11}^2[95y^2\zeta_{13}^2 + 6\zeta_{13}\left(75\upsilon^4 + 10\nu y\zeta_{21} - 6\mu\upsilon\zeta_{24}\right) + 180\nu^2\zeta_{21}^2] \\
&+4y^2\zeta_{11}^4[y\left(17y\zeta_{13} - 60\nu\zeta_{21}\right) + 270\upsilon\left(\upsilon^3 - 2\mu\zeta_{24}\right)] + 1080\zeta_{11}^3[\upsilon^2 y^2\zeta_{13} \\
&+2\nu\upsilon^2 y\zeta_{21} + \left(\upsilon^3 + \mu\zeta_{24}\right)^2] - 150\upsilon^2\zeta_{13}^2\zeta_{11} + 75\zeta_{13}^3]^2],
\end{aligned}
\tag{13}
$$

where ζ_{11}, ζ_{13}, ζ_{21} and ζ_{24} are unrestricted. Dynamic features of 3-rogue wave solutions are displayed in Figs. 3, 4, 5 and 6 when (μ, ν) selects different values, we can see that three rogue waves break apart and form a set of three 1-rogue waves in Figs. 3, 4, 5 and 6.

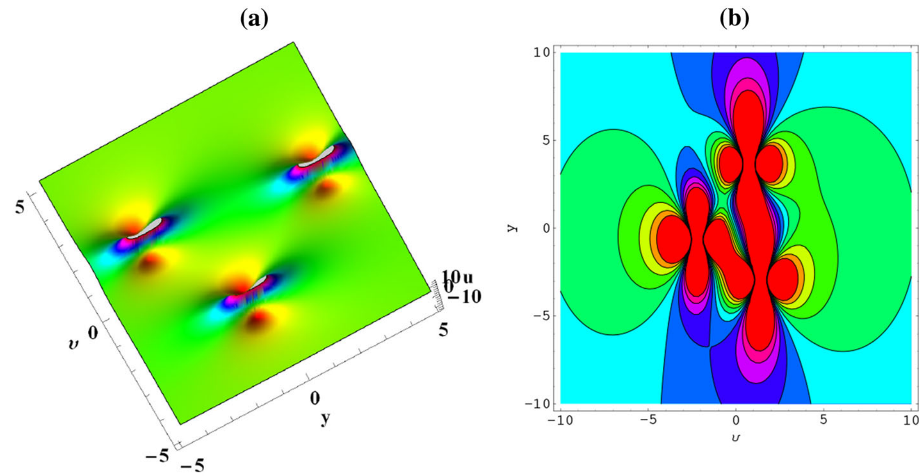

FIG. 6. Rogue wave (13) with $\mu = \nu = 10$, $\zeta_{11} = \zeta_{13} = \zeta_{21} = \zeta_{24} = 1$, $\Theta_0 = 1$, **a** 3D graphic, **b** contour plot

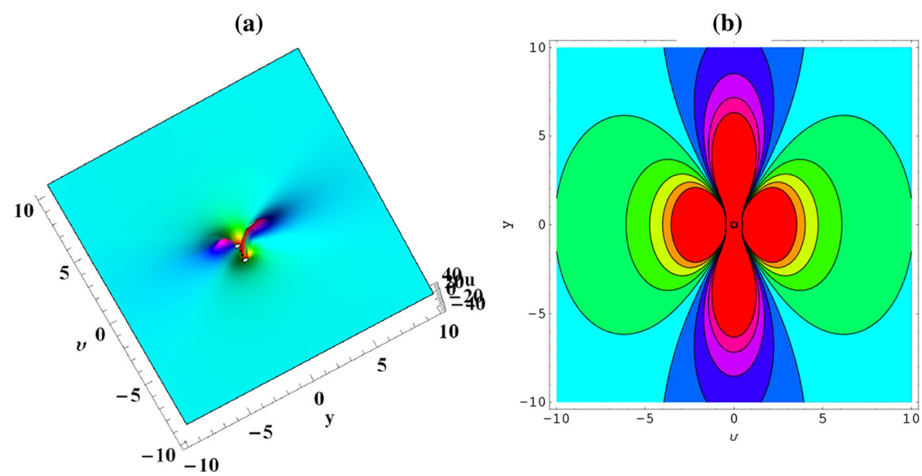

FIG. 7. Rogue wave (16) with $\mu = \nu = 0$, $\Theta_0 = 1$, $\zeta_0 = \zeta_1 = \zeta_{28} = 1$, $\zeta_{26} = 2$, **a** 3D graphic, **b** contour plot

5. 6-Rogue wave solutions

To present the 6-rogue wave solutions, we assume

$$\begin{aligned}\xi(\upsilon, y) = {} & \upsilon^{12} + y^8\zeta_{48} + y^6\zeta_{47} + y^4\zeta_{46} + \upsilon^{10}\left(y^2\zeta_{26} + \zeta_{25}\right) \\ & + y^2\zeta_{45} + \upsilon^8\left(y^4\zeta_{29} + y^2\zeta_{28} + \zeta_{27}\right) + 2\mu\upsilon[\upsilon^6 + y^6\zeta_{64} + y^4\zeta_{63} \\ & + \upsilon^4\left(y^2\zeta_{69} + \zeta_{68}\right) + y^2\zeta_{62} + \upsilon^2\left(y^4\zeta_{67} + y^2\zeta_{66} + \zeta_{65}\right) + \zeta_{61}] \\ & + 2\nu y[y^6 + y^4\left(\upsilon^2\zeta_{57} + \zeta_{56}\right) + y^2\left(\upsilon^4\zeta_{55} + \upsilon^2\zeta_{54} + \zeta_{53}\right) + \upsilon^6\zeta_{60} \\ & + \upsilon^4\zeta_{59} + \upsilon^2\zeta_{58} + \zeta_{52}] + \upsilon^6\left(y^6\zeta_{33} + y^4\zeta_{32} + y^2\zeta_{31} + \zeta_{30}\right)\end{aligned}$$

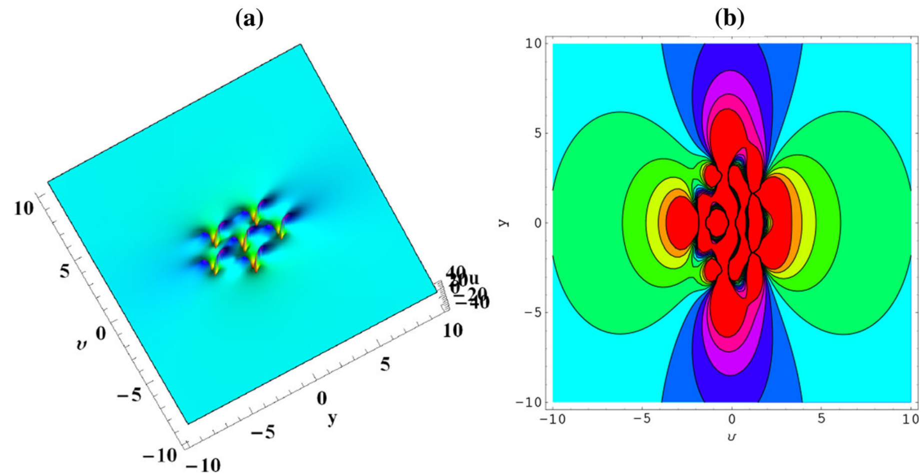

FIG. 8. Rogue wave (16) with $\mu = 10, \nu = 0$, $\Theta_0 = 1$, $\zeta_0 = \zeta_1 = \zeta_{28} = 1$, $\zeta_{26} = 2$, **a** 3D graphic, **b** contour plot

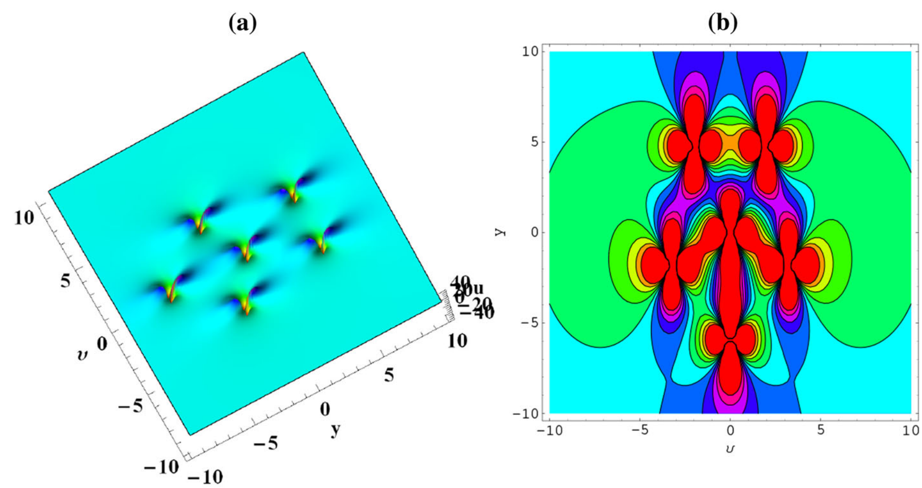

FIG. 9. Rogue wave (16) with $\mu = 0, \nu = 10$, $\Theta_0 = 1$, $\zeta_0 = \zeta_1 = \zeta_{28} = 1$, $\zeta_{26} = 2$, **a** 3D graphic, **b** contour plot

$$
\begin{aligned}
&+\upsilon^4\left(y^8\zeta_{38} + y^6\zeta_{37} + y^4\zeta_{36} + y^2\zeta_{35} + \zeta_{34}\right) + \upsilon^2(y^{10}\zeta_{44} + y^8\zeta_{43}\\
&+y^6\zeta_{42} + y^4\zeta_{41} + y^2\zeta_{40} + \zeta_{39}) + \zeta_{51} + y^{12}\zeta_{50} + y^{10}\zeta_{49}\\
&+\left(\mu^2 + \nu^2\right)[\upsilon^2 + y^2\zeta_1 + \zeta_0],
\end{aligned}
\tag{14}
$$

where $\zeta_i (i = 25, \ldots, 69)$ is unknown real constant. Substituting Eq. (14) into Eq. (7) and equating the coefficients of all powers υ and y to zero, we obtain

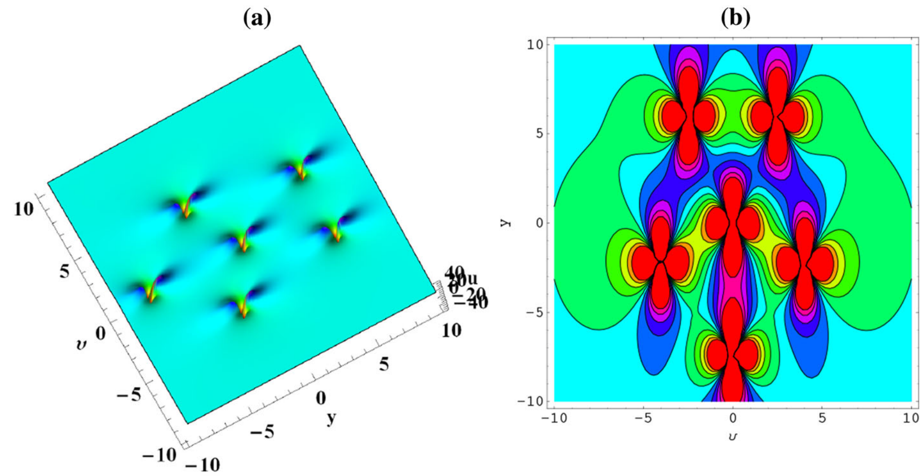

FIG. 10. Rogue wave (16) with $\mu = \nu = 30$, $\Theta_0 = 1$, $\zeta_0 = \zeta_1 = \zeta_{28} = 1$, $\zeta_{26} = 2$, **a** 3D graphic, **b** contour plot

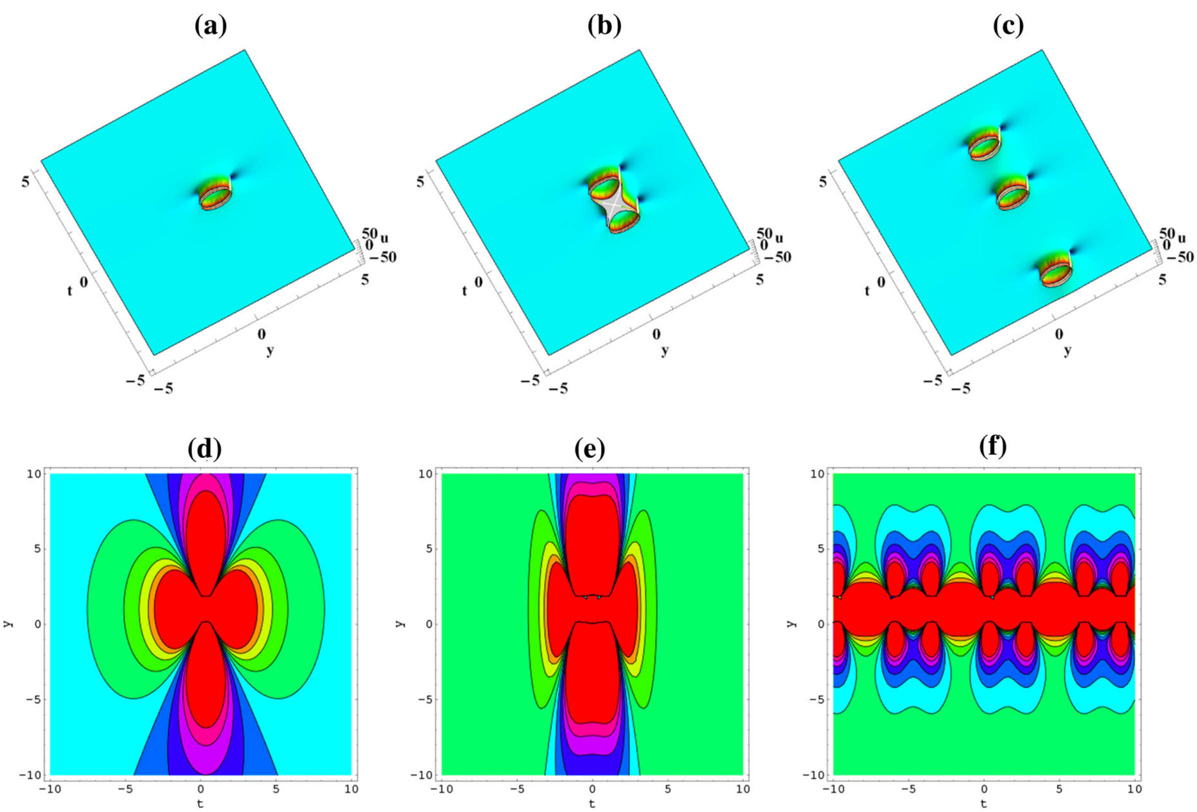

FIG. 11. Rogue wave (17) with $\mu = \nu = \Theta_0 = 1$, $x = 0$, $\zeta_0 = -1$, $\zeta_1 = 2$, $\beta(t) = 1$ in **a**, **d**, $\beta(t) = t$ in **b**, **e** and $\beta(t) = \cos t$ in **c**, **f**

$$
\begin{aligned}
\gamma(t) &= \frac{690\beta(t)}{\zeta_{28}}, \omega'(t) = \frac{1}{6}\zeta_{26}\gamma(t), \zeta_{29} = \frac{5\zeta_{26}^2}{12}, \zeta_{33} = \frac{5\zeta_{26}^3}{54},\\
\zeta_{32} &= \frac{77\zeta_{26}\zeta_{28}}{207}, \zeta_{31} = \frac{1862\zeta_{28}^2}{7935\zeta_{26}}, \zeta_{37} = \frac{73\zeta_{26}^2\zeta_{28}}{1242}, \zeta_{36} = \frac{749\zeta_{28}^2}{9522},\\
\zeta_{55} &= -\frac{180}{\zeta_{26}^2}, \zeta_{38} = \frac{5\zeta_{26}^4}{432}, \zeta_{35} = \frac{294\zeta_{28}^3}{12167\zeta_{26}^2}, \zeta_{43} = \frac{19\zeta_{26}^3\zeta_{28}}{4968},\\
\zeta_{42} &= \frac{77\zeta_{26}\zeta_{28}^2}{6210}, \zeta_{41} = -\frac{49\zeta_{28}^3}{182505\zeta_{26}}, \zeta_{52} = \frac{271656\zeta_{28}^3}{304175\zeta_{26}^6},\\
\zeta_{54} &= -\frac{1368\zeta_{28}}{23\zeta_{26}^3}, \zeta_{44} = \frac{\zeta_{26}^5}{1296}, \zeta_{57} = -\frac{54}{\zeta_{26}}, \zeta_{40} = \frac{3773\zeta_{28}^4}{6996025\zeta_{26}^3},\\
\zeta_{50} &= \frac{\zeta_{26}^6}{46656}, \zeta_{49} = \frac{29\zeta_{26}^4\zeta_{28}}{447120}, \zeta_{48} = \frac{289\zeta_{26}^2\zeta_{28}^2}{1142640},\\
\zeta_{64} &= \frac{5\zeta_{26}^3}{216}, \zeta_{47} = \frac{39949\zeta_{28}^3}{49276350}, \zeta_{27} = \frac{147\zeta_{28}^2}{2645\zeta_{26}^2},\\
\zeta_{67} &= -\frac{5\zeta_{26}^2}{36}, \zeta_{63} = \frac{\zeta_{26}\zeta_{28}}{92}, \zeta_{66} = -\frac{\zeta_{28}}{3},\\
\zeta_{25} &= \frac{98\zeta_{28}}{115\zeta_{26}}, \zeta_{56} = -\frac{42\zeta_{28}}{115\zeta_{26}^2}, \zeta_{46} = \frac{655669\zeta_{28}^4}{755570700\zeta_{26}^2},\\
\zeta_{53} &= -\frac{1764\zeta_{28}^2}{2645\zeta_{26}^4}, \zeta_{60} = \frac{1080}{\zeta_{26}^3}, \zeta_{69} = -\frac{3\zeta_{26}}{2}, \zeta_{65} = -\frac{49\zeta_{28}^2}{2645\zeta_{26}^2},\\
\zeta_{30} &= \frac{15092\zeta_{28}^3}{912525\zeta_{26}^3}, \zeta_{39} = -\nu^2 + \frac{279936\nu^2}{\zeta_{26}^7} + \frac{6391462\zeta_{28}^5}{2413628625\zeta_{26}^5},\\
\zeta_{34} &= -\frac{41503\zeta_{28}^4}{4197615\zeta_{26}^4}, \zeta_{68} = \frac{13\zeta_{28}}{115\zeta_{26}}, \zeta_{58} = -\frac{28728\zeta_{28}^2}{2645\zeta_{26}^5},\\
\zeta_{45} &= -\zeta_1\left(\mu^2+\nu^2\right) + \frac{\mu^2\zeta_{26}}{6} + \frac{46656\nu^2}{\zeta_{26}^6} + \frac{1203587\zeta_{28}^5}{1448177175\zeta_{26}^4},\\
\zeta_{62} &= \frac{107\zeta_{28}^2}{15870\zeta_{26}}, \zeta_{61} = \frac{2401\zeta_{28}^3}{912525\zeta_{26}^3}, \zeta_{59} = \frac{4536\zeta_{28}}{23\zeta_{26}^4},\\
\zeta_{51} &= \frac{3\zeta_{28}\left(279936\nu^2+\mu^2\zeta_{26}^7\right)}{115\zeta_{26}^8} - \zeta_0\left(\mu^2+\nu^2\right) + \frac{35153041\zeta_{28}^6}{832701875625\zeta_{26}^6}.
\end{aligned} \tag{15}
$$

Substituting Eqs. (14) and (15) into Eq. (6), the 6-rogue wave solutions for Eq. (1) can be written as

$$
u = 2\Theta_0\left(\frac{\xi_{\upsilon\upsilon}}{\xi} - \frac{\xi_\upsilon^2}{\xi^2}\right), \tag{16}
$$

where ξ satisfies Eq. (14) and Eq. (15), ζ_{26} and ζ_{28} are unrestricted. Dynamic features of 6-rogue wave solutions are shown in Figs. 7, 8, 9 and 10 when (μ, ν) selects different values, we can see that sixrogue waves break apart and form a set of six 1-rogue waves in Figs. 7, 8, 9 and 10.

6. Conclusion

In the paper, a variable-coefficient symbolic computation approach is proposed. The main difference between this method and the previous one in Ref. [18] is that we replace the traveling wave transformation with the non-traveling wave transformation, making it suitable for solving the multiple rogue wave solution of the nonlinear system with variable coefficients. This change has not been seen in other literatures. Applied the vcsca to the (2+1)-dimensional vcKP equation, the 1-rogue wave solutions, 3-rogue wave solutions and 6-rogue wave solutions are present. By setting different values of (μ, ν), their dynamic features are displayed in Figs. 1, 2, 3, 4, 5, 6, 7, 8, 9 and 10. All the obtained solutions have been verified to be correct.

Substituting $\upsilon = x - \omega(t)$ in rogue wave solution (10), we have

$$u(x,y,z,t) = \frac{4\Theta_0\left[-\left[\mu + \frac{3\int \beta(t)\,dt}{\zeta_0} - x\right]^2 + \zeta_1(y-\nu)^2 + \zeta_0\right]}{\left[\left[\mu + \frac{3\int \beta(t)\,dt}{\zeta_0} - x\right]^2 + \zeta_1(y-\nu)^2 + \zeta_0\right]^2}. \tag{17}$$

When variable-coefficient $\beta(t)$ chooses different function, the rogue wave (17) shows different dynamic features in Fig. 11.

In addition to this (2+1)-dimensional vcKP equation, this vcsca can also be applied to the (3+1)-dimensional generalized KP equation with variable coefficients [22], the generalized (3 + 1)-dimensional variable-coefficient nonlinear wave equation [23] based on the symbolic computation [24–36].

Declarations

Conflict of interest The authors declare that there is no conflict of interests regarding the publication of this article.

Ethical standard The authors state that this research complies with ethical standards. This research does not involve either human participants or animals.

Publisher's Note Springer Nature remains neutral with regard to jurisdictional claims in published maps and institutional affiliations.

References

[1] Wang, Y.Y., Zhang, J.F.: Variable-coefficient KP equation and solitonic solution for two-temperature ions in dusty plasma. Phys. Lett. A. **352**(1), 155–162 (2006)
[2] Yao, Z.Z., Zhang, C.Y., et al.: Wronskian and grammian determinant solutions for a variable-coefficient Kadomtsev-Petviashvili equation. Commun. Theor. Phys. **49**(5), 1125–1128 (2008)
[3] Wu, J.P.: Bilinear Bäcklund transformation for a variable-coefficient Kadomtsev-Petviashvili equation. Chin. Phys. Lett.s **28**(6), 060207 (2011)
[4] Liu, J.G., Zhu, W.H., Zhou, L.: Breather wave solutions for the Kadomtsev-Petviashvili equation with variable coefficients in a fluid based on the variable-coefficient three-wave approach. Math. Method. Appl. Sci. **43**(1), 458–465 (2020)
[5] Jia, X.Y., Tian, B., Du, Z., Sun, Y., Liu, L.: Lump and rogue waves for the variable-coefficient Kadomtsev-Petviashvili equation in a fluid. Mod. Phys. Lett. B **32**(10), 1850086 (2018)
[6] Liu, J.G., Zhu, W.H., Zhou, L.: Interaction solutions for Kadomtsev-Petviashvili equation with variable coefficients. Commun. Theor. Phys. **71**, 793–797 (2019)
[7] Grimshaw, R., Pelinovsky, E., Taipova, T., Sergeeva, A.: Rogue internal waves in the ocean: long wave model. Eur. Phys. J. Spec. Top. **185**, 195–208 (2010)
[8] Zuo, D.W., Gao, Y.T., Xue, L., Feng, Y.J., Sun, Y.H.: Rogue waves for the generalized nonlinear Schrödinger-Maxwell-Bloch system in optical-fiber communication. Appl. Math. Lett. **40**, 78–83 (2015)
[9] He, J.S., Charalampidis, E.G., Kevrekidis, P.G., Frantzeskakis, D.J.: Rogue waves in nonlinear Schrödinger models with variable coefficients: application to Bose-Einstein condensates. Phys. Lett. A **378**(5–6), 577–583 (2014)
[10] Li, B.Q., Ma, Y.L.: Rogue waves for the optical fiber system with variable coefficients. Optik **158**, 177–184 (2018)
[11] Ma, W.X.: Lump and interaction solutions to linear PDEs in 2+1 dimensions via symbolic computation. Mod. Phys. Lett. B **33**, 1950457 (2019)
[12] Ankiewicz, A., Akhmediev, N.: Rogue wave-type solutions of the mKdV equation and their relation to known NLSE rogue wave solutions. Nonlinear Dyn. **91**(3), 1931–1938 (2018)
[13] Ma, W.X., Zhang, L.Q.: Lump solutions with higher-order rational dispersion relations. Pramana-J. Phys. **94**, 43 (2020)

[14] Su, J.J., Gao, Y.T., Ding, C.C.: Darboux transformations and rogue wave solutions of a generalized AB system for the geophysical flows. Appl. Math. Lett. **88**, 201–208 (2019)

[15] Wang, X.B., Zhang, T.T., Dong, M.J.: Dynamics of the breathers and rogue waves in the higher-order nonlinear Schrödinger equation. Appl. Math. Lett. **86**, 298–304 (2018)

[16] Liu, J.G., You, M.X., Zhou, L., Ai, G.P.: The solitary wave, rogue wave and periodic solutions for the (3+1)-dimensional soliton equation. Z. Angew. Math. Phys. **70**, 4 (2019)

[17] Clarkson, P.A., Dowie, E.: Rational solutions of the Boussinesq equation and applications to rogue waves. Trans. Math. Appl. **1**(1), tnx003 (2017)

[18] Zha, Q.L.: A symbolic computation approach to constructing rogue waves with a controllable center in the nonlinear systems. Comput. Math. Appl. **75**(9), 3331–3342 (2018)

[19] Liu, W.H., Zhang, Y.F.: Multiple rogue wave solutions of the (3+1)-dimensional Kadomtsev-Petviashvili-Boussinesq equation. Z. Angew. Math. Phys. **70**, 112 (2019)

[20] Zhao, Z.L., He, L.C., Gao, Y.B.: Rogue wave and multiple lump solutions of the (2+1)-dimensional Benjamin-Ono equation in fluid mechanics. Complexity **2019**, 8249635 (2019)

[21] Liu, W.H., Zhang, Y.F.: Multiple rogue wave solutions for a (3+1)-dimensional Hirota bilinear equation. Appl. Math. Lett. **98**, 184–190 (2019)

[22] Liu, J.G., Ye, Q.: Stripe solitons and lump solutions for a generalized Kadomtsev-Petviashvili equation with variable coefficients in fluid mechanics. Nonlinear Dyn. **96**(1), 23–29 (2019)

[23] Deng, G.F., Gao, Y.T.: Integrability, solitons, periodic and travelling waves of a generalized (3+1)-dimensional variable-coefficient nonlinear-wave equation in liquid with gas bubbles. Eur. Phys. J. Plus. **132**(6), 255–271 (2017)

[24] Gaillard, P.: Rational solutions to the KPI equation and multi rogue waves. Ann. Phys. **367**, 1–5 (2016)

[25] Yin, Y.H., Ma, W.X., Liu, J.G., Lü, X.: Diversity of exact solutions to a (3+1)-dimensional nonlinear evolution equation and its reduction. Comput. Math. Appl. **76**, 1275–1283 (2018)

[26] Lü, X., Lin, F.H., Qi, F.H.: Analytical study on a two-dimensional Korteweg-de Vries model with bilinear representation, Bäcklund transformation and soliton solutions. Appl. Math. Model. **39**, 3221–3226 (2015)

[27] Xu, G.Q., Wazwaz, A.M.: Characteristics of integrability, bidirectional solitons and localized solutions for a (3 + 1)-dimensional generalized breaking soliton equation. Nonlinear Dyn. **96**, 1989–2000 (2019)

[28] Ma, W.X., Mousa, M.M., Ali, M.R.: Application of a new hybrid method for solving singular fractional LaneCEmden-type equations in astrophysics. Mod. Phys. Lett. B **34**(3), 2050049 (2020)

[29] Ren, B., Ma, W.X., Yu, J.: Lump solutions for two mixed Calogero-Bogoyavlenskii-Schiff and Bogoyavlensky-Konopelchenko equations. Commun. Theor. Phys. **71**(6), 658–662 (2019)

[30] Li, Y.Z., Liu, J.G.: New periodic solitary wave solutions for the new (2+1)-dimensional Korteweg-de Vries equation. Nonlinear Dyn. **91**(1), 497–504 (2018)

[31] Ma, W.X.: Global behavior of a new rational nonlinear higher-order difference equation. Complexity **2019**, 2048941 (2019)

[32] Lan, Z.Z., Su, J.J.: Solitary and rogue waves with controllable backgrounds for the non-autonomous generalized AB system. Nonlinear Dyn. **96**, 2535–2546 (2019)

[33] Chen, S.J., Yin, Y.H., Ma, W.X., Lü, X.: Abundant exact solutions and interaction phenomena of the (2 + 1)-dimensional YTSF equation. Anal. Math. Phys. **9**, 2329–2344 (2019)

[34] Ma, W.X.: Interaction solutions to Hirota-Satsuma-Ito equation in (2 + 1)-dimensions. Front. Math. China **14**, 619–629 (2019)

[35] Ma, W.X.: Lump solutions to the Kadomtsev-Petviashvili equation. Phys. Lett. A **379**, 1975–1978 (2015)

[36] Ma, W.X., Zhou, Y.: Lump solutions to nonlinear partial differential equations via Hirota bilinear forms. J. Differ. Equ. **264**, 2633–2659 (2018)

Jian-Guo Liu and Yan He
College of Computer
Jiangxi University of Chinese Medicine
Nanchang 330004 Jiangxi
China
e-mail: 395625298@qq.com

Jian-Guo Liu
School of science
Beijing University of Posts and Telecommunications
Beijing 100876
China

Wen-Hui Zhu
Institute of artificial intelligence
Nanchang Institute of Science and Technology
Nanchang 330108 Jiangxi
China
e-mail: 415422402@qq.com

(Received: December 19, 2019; revised: May 9, 2020; accepted: June 23, 2021)